

CDMA Downlink Transmission with Transmit Antenna Arrays and Power Control in Multipath Fading Channels^{*}

Huaiyu Dai^{*}, *Member, IEEE*, Laurence Mailaender, and H. Vincent Poor, *Fellow, IEEE*⁺

Abstract

Wireless code-division multiple-access (CDMA) cellular downlink communications with transmit antenna arrays in multipath fading channels is studied. Various array signal processing techniques at the transmit end are investigated and compared under various settings, in conjunction with power control. No instant downlink channel information is assumed; however, the obtained results are also compared with results assuming ideal feedback. The study is carried out for both circuit-switched and packet-switched systems, where different goals are pursued and different conclusions are drawn. In particular, it is found that traffic type impacts the algorithm choice in downlink transmission, and that there is no need to seek optimum power control/allocation schemes, which are either too complex or infeasible in practice. Another interesting conclusion is that, even though feedback does not help much for packet-switched systems, it does help for circuit-switched systems, the gain of which increases with the number of antennas.

Index Terms: CDMA, downlink transmission, multipath fading, power control, transmit arrays

^{*} This research was supported in part by Bell Labs, Lucent Technologies, in part by the National Science Foundation under Grant CCR 99-80590, and in part by the New Jersey Center for the Wireless Telecommunications.

⁺ H. Dai was with the Department of Electrical Engineering, Princeton University. He is now with the Department of Electrical and Computer Engineering, NC State University, Raleigh, NC 27695-7511. Phone: (919) 513-0299; Fax: (919) 515-2285; Email: Huaiyu_Dai@ncsu.edu. H. V. Poor is with the Department of Electrical Engineering, Princeton University, Princeton, NJ 08544. Email: poor@princeton.edu. L. Mailaender is with the Wireless Communications Research Department, Bell Labs, Lucent Technologies, Holmdel, NJ 07733. Email: lm@lucent.com. Part of this work was done while H. Dai was a summer intern with Bell Labs, Lucent Technologies.

I. Introduction

Cellular base stations may make use of an antenna array to achieve diversity gains or antenna gains so as to improve the system capacity. In a fading environment, the antenna elements should be separated sufficiently far apart to experience uncorrelated fading and to thereby achieve the diversity gain [21]. In urban areas, the required spacing is half a wavelength at the mobile and ten times a wavelength at the base station. Independent of the fading environment and in addition to the diversity gain, multiple antennas can provide antenna gain due to the potential coherent combining of the transmitted and/or received signals and the underlying uncorrelated noise. This technique is usually called beamforming, where the signals are modeled as planar wavefronts impinging on/transmitting from an antenna array with a certain direction of arrival (DOA)/direction of departure (DOD) [16]. In the beamforming approach, the antenna elements are usually closely spaced so that correlated fading coefficients are obtained for the elements of an antenna array, which form a vector called the spatial signature or the steering vector. The spatial signature, analogous to the spreading signature in the direct-sequence code-division multiple-access (DS-CDMA) systems, is often exploited for interference suppression. In this study, we focus on array processing techniques to improve the CDMA cellular downlink transmission, which is foreseen to be of crucial importance for the next generation communication systems supporting wireless Internet, video on demand, and multimedia services. In particular, we will determine the optimal transmission schemes for both voice and data applications, and investigate the influence of the feedback and number of antennas.

Perhaps the simplest form of spatial processing is open loop transmit diversity, which will serve as the performance baseline in this study. Sectorization, which can be interpreted as fixed beam transmission, is well known to be an effective way to improve the system capacity [13]. Other array processing techniques discussed in this paper belong to the beamforming category. A simple form of transmit beamforming is beam steering, which assumes knowledge of the mobile's position and forms a beam in the direction of line-of-sight. The performance of beam steering degrades in multipath channels with angle spread. A more sophisticated use of the array is to determine the antenna-weighting vector that

maximizes signal-to-noise ratio (SNR) at the mobiles. Alternatively, one can borrow the idea from uplink receive array processing and come up with a maximum signal-to-interference ratio (SIR) solution for weighting vector design, i.e., maximizing the ratio of the received power of the signal at the desired user and that leaked to the other users. Note that the downlink communication scenario is different from that of the uplink. While in the uplink the weighting vector designs for different users are de-coupled, optimal beamforming for the downlink will have to be considered jointly, because the weighting vector for one user will impact the interference received by other users as well as the useful signal power received by the desired user. A joint power control and downlink beamforming algorithm has been proposed in [14] and [18] according to some optimality criterion, and will also be used as the performance baseline.

Power control was conceived originally as a mechanism to deal with the near-far problem, but a more general emerging view is that it is a flexible mechanism to provide different quality-of-service to users with heterogeneous requirements [6]. For downlink transmission, power control is also important for energy conservation and interference mitigation. In circuit-switched systems, when we perform the above downlink transmission array processing together with power control, we execute it in two steps: 1) an array weighting vector is determined (not needed for transmit diversity) and the signal-to-interference-and-noise ratio (SINR) is calculated (as functions of transmitted powers) for each mobile receiver; 2) transmitted power is allocated among users so as to minimize the total transmitted power from the base station while keeping the SINRs of all links above a certain threshold. When there is no feasible solution for power allocation or the total transmitted power needed exceeds the maximum threshold, an outage is declared. The figure of merit for circuit-switched systems is the (simultaneously) supportable user capacity with certain SINR requirement under some outage limit. However, in packet-switched systems (such as HDR or HSDPA), where users are delay tolerant, we carry out rate control instead of power control, assuming the base station transmits at its maximum power. We mainly assume the powers are equally allocated among active users; but an optimal power allocation scheme will also be studied. The figure of merit for the packet-switched systems is the total throughput (data rate), which is directly related to the SINR seen at the mobile users. Throughout this paper, no instant downlink channel state

information (CSI) is assumed; however, the obtained results are also compared with results assuming ideal CSI. Both systems have a total transmit power constraint.

This paper is organized as follows: in Section II the system model is introduced. Power control/allocation algorithms for circuit/packet switched systems are addressed in Section III under a common framework. In Section IV, various transmit array-processing techniques are presented, in conjunction with power control. Section V provides numerical comparison results for these array processing techniques under various settings for both circuit-switched and packet-switched systems. Section VI concludes the paper.

II. System Model

A. Multipath Channel

We assume a CDMA frequency division duplex (FDD) cellular system. In each cell K mobile users, each employing a single antenna, communicate with a base station having an M -element antenna array. The spreading codes employed within a cell by different users, or different antenna elements and different users (for code transmit diversity) are assumed to be mutually orthogonal with spreading gain N ; while any two codes (either identical or different) with different delays (for different paths) are assumed to be independent. The physical channel between the mobile users and the base station is assumed to be wide sense stationary with uncorrelated scattering (WSSUS) multipath frequency-selective fading. We assume for simplicity that there are L paths for each user.

For the beamforming techniques, after joint transmission of the weighted signals bound for different users from the base station, the baseband signal received by the i th mobile user is given by

$$r_i(t) = \sqrt{G_i} \sum_{k=1}^K \sqrt{P_k} b_k \mathbf{w}_k^H \sum_{l=1}^L \alpha_{il}^D(t) \mathbf{a}^D(\theta_{il}) c_k(t - \tau_{il}) + n_i(t), \quad (1)$$

where P_k is the power assigned to the user k ; b_k is the transmitted data for user k ; \mathbf{w}_k is the transmit beamforming weight vector for user k ; $c_k(t)$ is the spreading waveform assigned to user k ; G_i is the path gain from the transmit array to the i th user, which combines the effects of path loss and shadowing; τ_{il} is

the delay of the l th path from the base-station antenna array to the i th user; $\alpha_{il}^D(t)$ describes the small-scale fading random process of the l th path from the base-station antenna array to the i th user, which is frequency dependent and largely uncorrelated for uplink and downlink; and θ_{il} is the angle of departure of the l th path from the base-station antenna array to the i th user. In our model, we assume that θ_{il} , $1 \leq l \leq L$, has a Gaussian distribution centered at $\theta_{i,los}$, the line-of-sight (LOS) direction from the base-station antenna array to the i th user. With the assumptions of planar waves and a uniform linear array, the frequency dependent downlink steering vector is given by

$$\mathbf{a}^D(\theta_{il}) = \left[1, e^{-j2\pi d_a \frac{f_D}{c} \sin(\theta_{il})}, \dots, e^{-j2\pi d_a (M-1) \frac{f_D}{c} \sin(\theta_{il})} \right]^T, \quad (2)$$

where d_a is the inter-element spacing of the antenna array and f_D is the downlink carrier frequency. Finally, $n_i(t)$ is the noise term, which includes the thermal background noise and the out-of-cell interference, to be further addressed in the sequel. In this paper, we are mainly interested in a chip-matched-filtered and chip-sampled discretized model, easily derived from (1) as

$$\mathbf{r}_i = \sqrt{G_i} \sum_{k=1}^K \sqrt{P_k} b_k \mathbf{w}_k^H \sum_{l=1}^L \alpha_{il}^D \mathbf{a}_{il}^D \mathbf{c}_k^{il} + \mathbf{n}_i, \quad (3)$$

where the length of the received vector is large enough to catch the signals from all L paths. We assume that the path delay is negligible compared to the spreading length, so that intersymbol interference (ISI) can be ignored.

While the base-station antenna elements should be closely spaced for beamforming techniques to get coherent signals across the antenna array, they should be widely separated to get diversity gain for transmit diversity schemes. Rather than being combined with a steering vector, the signals coming from different elements of an antenna array exploiting transmit diversity experience uncorrelated fading. Assuming a simple code transmit diversity scheme without code reuse¹, the transmitted signal from the m th antenna can be modeled as

¹ A total of KM Walsh codes are required. To conserve codes, techniques such as space-time spreading [7] can be used, but the performance achieved is not different.

$$s_m(t) = \frac{1}{\sqrt{M}} \sum_{k=1}^K \sqrt{P_k} b_k c_{km}(t), \quad (4)$$

where $c_{km}(t)$ is the spreading code for the k th user in the m th antenna, and the total transmitted energy of one user is normalized with the number of transmit antennas. Note that while beamforming techniques applies different weights for each antenna element on the signals of one user, (code) transmit diversity assigns different spreading codes for each antenna element to the signals of one user. For the transmit diversity technique, the received signal at the i th mobile is given by

$$r_i(t) = \sqrt{\frac{G_i}{M}} \sum_{m=1}^M \sum_{k=1}^K \sqrt{P_k} b_k \sum_{l=1}^L \alpha_{ml}^i c_{km}(t - \tau_{il}) + n_i(t), \quad (5)$$

where it is noted that for each path of the multipath channels between each antenna element and the mobile user, even though the delays are not significantly different across the array, the instantaneous fading coefficients $\{\alpha_{ml}^i\}$ are uncorrelated. The other elements of (5) are self-explanatory. Again, it is preferable to deal with the discretized model given as

$$\mathbf{r}_i = \sqrt{\frac{G_i}{M}} \sum_{m=1}^M \sum_{k=1}^K \sqrt{P_k} b_k \mathbf{C}_{km}^i \mathbf{h}_m^i + \mathbf{n}_i, \quad (6)$$

where $\mathbf{C}_{km}^i = [\mathbf{c}_{km}^{i1}, \dots, \mathbf{c}_{km}^{iL}]$, whose columns are discretized delayed versions of $c_{km}(t)$ corresponding to different paths, and $\mathbf{h}_m^i = [\alpha_{m1}^i, \dots, \alpha_{mL}^i]^T$ collects the instantaneous small-scale fading coefficients of the L paths from the m th antenna to the i th user.

B. FDD Framework

In FDD systems, the separation between the uplink and downlink carrier frequencies is large enough to reject the reciprocity principle. However, if the frequency separation is not too large, the uplink and downlink will still share many common features, among which are the number of radio paths, their delays and angles, the large-scale path loss and shadowing, and the variance of small-scale fading [11], [12]. Nevertheless, the instantaneous small-scale fading of the two links is uncorrelated, which makes the downlink problem more difficult for FDD systems. The signal received at the base station provides a means for directly estimating the uplink, not the downlink channel. While such information could be

available via a feedback channel from the mobile, we assume that no such channel exists. The fact that the array response is also frequency dependent further complicates the problem.

Although the small-scale fading is uncorrelated between the uplink and downlink, their average strength is assumed to be insensitive to small changes in frequency [8], [12], i.e.,

$$E\{|\alpha_{kl}^D|^2\} = E\{|\alpha_{kl}^U|^2\}, \quad (7)$$

where the superscript ‘‘D’’ and ‘‘U’’ denote downlink and uplink, respectively. Therefore, the long-term statistics of the downlink small-scale fading can be estimated via time average from uplink data. To estimate the downlink steering vectors, several approaches exist. One idea (the matched array) is to design two separate closely-located arrays which are scaled versions of each other in proportion to the ratio of the uplink and downlink wavelengths, thus making the uplink and downlink steering vectors the same [12]. The drawbacks of this approach are cost, imperfect array matching and near field uneven scattering. A clever log-periodic array configuration is proposed in [8], which overlaps the two subarrays of M elements mentioned above into one $M + 1$ array with $d_m / d_{m-1} = \lambda_U / \lambda_D$, where d_m is the spacing between the m th and the $(m + 1)$ th element. The drawbacks above are alleviated but still exist. Another approach (the duplex array) is to use a single array for both the uplink and downlink, and to transpose the array response from the uplink to the downlink via a linear transformation. However, some constraints are imposed to make the linear transformation tractable, e.g., a small frequency shift assumption in [12] and circular array geometry in [1]. In our work, we exploit the approach of estimating the DODs from the uplink data through high-resolution DOA estimation methods or training sequences, assuming reciprocity principle holds for DODs and DOAs. We also ignore the estimation errors, which deserves further study. Then the downlink steering vector is calculated through (2). In the sequel, the superscript ‘‘D’’ will be omitted for the beamforming model (3) when no ambiguity is incurred.

Throughout this paper, we assume that the downlink channel is known at the receiver, but only approximated at the transmitter.

C. Cellular System

We consider a cellular geometry as shown in Fig. 1. It consists of two tiers of surrounding cells around the cell of interest. Each cell is divided into three sectors of 120 degrees unless otherwise indicated. Because CDMA is explored, mobile users in the sector of interest will suffer interference from adjacent sectors of the same cell, as well as from surrounding cells, as indicated in Fig. 1. For simplicity, the out-of-cell/sector interference is assumed to be white and Gaussian and is included in the noise term of the model, so that only its power matters. Throughout this paper, we assume the noise vector seen at mobile i is complex Gaussian with independent and identically distributed (i.i.d.) components of zero mean and variance σ_i^2 . We assume that all cells and sectors are identical, which are loaded with the same number of users exhibiting the same behavior, and at the base stations the same operations are exploited. This model should reflect the average performance of actual systems in the long run.

III. Power Control/Allocation Algorithms

In different application scenarios, optimal power control/allocation may have different meanings. For a circuit-switched system, a commonly used criterion is formulated as follows:

$$\min \sum_{k=1}^K P_k \quad s.t. \quad \text{SINR}_k \geq \gamma_k, \quad 1 \leq k \leq K, \quad (8)$$

i.e., minimize the total transmitted power with the constraints that each link attains an SINR above a certain threshold. For a packet-switched system, we always transmit at the maximum power, and we are concerned with the throughput of the network. We can simply allocate power equally among the active users, or we can allocate power in some optimal way. An optimal power assignment scheme proposed in [23] is formulated as follows:

$$\max \text{SINR}_{\min} \quad s.t. \quad \sum_{k=1}^K P_k \leq P_{\max}, \quad (9)$$

i.e., maximize the minimum link SINR with the total transmitted power constraint. This scheme tries to be fair to all users, which is not necessarily a good strategy for maximal throughput without taking into consideration the data link budget and network schedule.

It turns out that these two power control/allocation schemes are related to the same algebraic theorem given as follows [10].

A. Perron-Frobenius Theorem and its Applications

Theorem: Suppose \mathbf{T} is an $n \times n$ non-negative² irreducible matrix. Then there exists an eigenvalue r such that:

- a. *r is real and positive;*
- b. *r is associated with strictly positive left and right eigenvectors;*
- c. *$r = \max\{|\lambda_i|\} = \rho(\mathbf{T})$, where $\lambda_i, 1 \leq i \leq n$ are the eigenvalues of the matrix \mathbf{T} , and $\rho(\mathbf{T})$ denotes its spectral radius;*
- d. *r has algebraic multiplicity 1;*
- e. *$\min_i \sum_{j=1}^n t_{ij} \leq r \leq \max_i \sum_{j=1}^n t_{ij}$ with equality on either side implying equality throughout. A similar result holds for column sums.*

Application 1: A necessary and sufficient condition for a non-negative (non-trivial³) solution \mathbf{x} to the equations $(s\mathbf{I} - \mathbf{T})\mathbf{x} = \mathbf{c}$ to exist for any nonnegative (non-trivial) vector \mathbf{c} is that $s > r$. In this case there is only one strictly positive solution given by $(s\mathbf{I} - \mathbf{T})^{-1}\mathbf{c}$.

Application 2: If a non-negative (non-trivial) vector \mathbf{y} satisfies $\mathbf{T}\mathbf{y} \leq s\mathbf{y} (s > 0)$, then $\mathbf{y} > 0$, $s \geq r$, and $s = r$ if and only if $\mathbf{T}\mathbf{y} = s\mathbf{y}$.

B. General Form of Power Control/Allocation Solutions

The power control criterion of (8) is related to Application 1 of the theorem as follows. The general form of the power control problem can be reformulated as

$$\min \sum_{k=1}^K P_k \quad s.t. \quad (\mathbf{I} - \mathbf{DF})\mathbf{p} = \mathbf{u}, \quad (10)$$

² Here the term nonnegative refers to a vector or matrix all of whose elements are nonnegative. The definition for strictly positive is similar.

³ A trivial vector or matrix is one having all-zero elements.

where \mathbf{I} is a K by K identity matrix, \mathbf{D} is a diagonal matrix with entries $\gamma_1, \dots, \gamma_K$, \mathbf{F} is a non-negative irreducible matrix (interference term), $\mathbf{p} = [P_1, P_2, \dots, P_K]^T$ collects the powers assigned to all users, and \mathbf{u} is a positive vector (noise term)⁴. So we have a feasible (non-negative) solution for the power allocation vector if and only if the spectral radius of \mathbf{DF} is less than one, otherwise we will claim an outage occurs. We call this a type-I outage and call the case in which we do get a non-negative solution but the total transmitted power exceeds the maximum threshold, i.e., $\mathbf{p}^T \mathbf{1} > P_{\max}$, a type-II outage. The solution to (10), if it exists, is given by $(\mathbf{I} - \mathbf{DF})^{-1} \mathbf{u}$ or alternatively by Jacobi iteration

$$\mathbf{p}^{(n+1)} = \mathbf{u} + \mathbf{DFp}^{(n)}, \quad (11)$$

which will converge for any initial value in this setting.

The power allocation criterion of (9) is related to Application 2 of the theorem as follows. It can easily be shown that this optimization scheme results in equal SINR = γ for all links. The objective functions then become

$$\mathbf{p} = \gamma(\mathbf{Fp} + \mathbf{h}) \quad \text{and} \quad \mathbf{p}^T \cdot \mathbf{1} = P_{\max}, \quad (12)$$

with $h_i = u_i / \gamma$. On writing $\mathbf{y} = [\mathbf{p}^T, 1]^T$, we can rewrite (12) as

$$\mathbf{T}\mathbf{y} = \gamma\mathbf{Q}\mathbf{y} \quad (13)$$

with

$$\mathbf{T} = \begin{bmatrix} \mathbf{I}_{K \times K} & \mathbf{0}_{K \times 1} \\ \mathbf{1}^T & -P_{\max} \end{bmatrix} \quad \text{and} \quad \mathbf{Q} = \begin{bmatrix} \mathbf{F} & \mathbf{h} \\ \mathbf{0}_{1 \times K} & 0 \end{bmatrix}, \quad (14)$$

where $\mathbf{1}$ is an all-1 vector. Alternatively, we can write it as

$$\mathbf{R}\mathbf{y} = \frac{1}{\gamma} \mathbf{y}, \quad (15)$$

with

⁴ Exact SINR formulas will be given in the next section, together with the definitions for \mathbf{F} and \mathbf{u} .

$$\mathbf{R} = \mathbf{T}^{-1}\mathbf{Q} = \begin{bmatrix} \mathbf{F} & \mathbf{h} \\ \mathbf{1}^T \mathbf{F} / P_{\max} & \mathbf{1}^T \mathbf{h} / P_{\max} \end{bmatrix}. \quad (16)$$

It is easily shown that \mathbf{R} is a non-negative irreducible matrix. So we always have a unique positive solution for \mathbf{p} and the SINR margin is the reciprocal of the largest eigenvalue of \mathbf{R} .

IV. Array Signal Processing

In this section, various array signal processing techniques are discussed in detail, among which are transmit diversity, sectorization, and beamforming techniques including beam steering, maximum SNR beamforming, and maximum SIR or SINR beamforming. We assume that the mobile receiver can learn the fading channel and perform RAKE combining. So the instantaneous SINR is obtained for each scheme, based on which the power control of Section III is then applied. A joint power control and beamforming algorithm [18] is also discussed, and its optimality is verified in our setting.

A. Transmit Diversity

We exploit code transmit diversity for downlink CDMA communications. The data streams of all users are transmitted simultaneously. For each user each data symbol is transmitted with equal power from every antenna using multiple mutually orthogonal spreading codes. On denoting $\mathbf{b} = [b_1, \dots, b_K]^T$,

$\tilde{\mathbf{I}}_{km}^i = \mathbf{C}_{km}^i \mathbf{h}_m^i$, $\mathbf{I}_k^i = \sum_{m=1}^M \tilde{\mathbf{I}}_{km}^i$, $\mathbf{L}^i = [\mathbf{I}_1^i, \dots, \mathbf{I}_K^i]$, and $\mathbf{P} = \sqrt{\frac{G_i}{M}} \text{diag}(\sqrt{P_1}, \dots, \sqrt{P_K})$, (6) can be rewritten as

$$\mathbf{r}_i = \mathbf{L}^i \mathbf{P} \mathbf{b} + \mathbf{n}_i. \quad (17)$$

A standard space-time RAKE receiver yields

$$(\mathbf{I}_i^i)^H \mathbf{r}_i = \sqrt{\frac{G_i}{M}} \sqrt{P_i} \{(\mathbf{I}_i^i)^H \mathbf{I}_i^i\} b_i + \sum_{k \neq i} \sqrt{\frac{G_i}{M}} \sqrt{P_k} \{(\mathbf{I}_i^i)^H \mathbf{I}_k^i\} b_k + \{(\mathbf{I}_i^i)^H \mathbf{n}_i\}. \quad (18)$$

Assuming that

$$\langle \mathbf{c}_{k1,m1}^{i,l1}, \mathbf{c}_{k2,m2}^{i,l2} \rangle = \begin{cases} 1 & l1 = l2, k1 = k2, m1 = m2 \\ 0 & l1 = l2, (k1, m1) \neq (k2, m2), \\ \beta & l1 \neq l2 \end{cases} \quad (19)$$

where β is a random variable with

$$E\{\beta\} = 0 \quad \text{and} \quad E\{\beta^2\} = \frac{1}{N}, \quad (20)$$

and on denoting

$$A^i = \sum_{m=1}^M \sum_{l=1}^L |\alpha_{ml}^i|^2 \quad (21)$$

and

$$C^i = \frac{1}{N} \sum_m \sum_{m'} \sum_l \sum_{l' \neq l} |\alpha_{ml}^i|^2 |\alpha_{m'l'}^i|^2, \quad (22)$$

the SINR for user i is given by

$$\text{SINR}_i = \frac{\frac{G_i}{M} P_i \left[(A^i)^2 + \frac{4}{N} \sum_m \sum_l \sum_{m'} \sum_{l' \neq l} \sum_{(m'-1)L+l' > (m-1)L+l} \text{Re}(\alpha_{ml}^i \alpha_{m'l'}^i)^2 \right]}{\sum_{k \neq i} \frac{G_i}{M} P_k C^i + \sigma_i^2 A^i} \approx \frac{\frac{G_i}{M} P_i (A^i)^2}{\sum_{k \neq i} \frac{G_i}{M} P_k C^i + \sigma_i^2 A^i}. \quad (23)$$

The power control formula (10) is exemplified here with

$$\mathbf{D} = \text{diag}(\gamma_1, \dots, \gamma_K), \quad (24)$$

$$F_{ij} = \begin{cases} 0 & i = j \\ \frac{C^i}{(A^i)^2} & i \neq j \end{cases}, \quad (25)$$

and

$$u_i = \frac{\gamma_i \sigma_i^2 M}{G_i A^i}. \quad (26)$$

B. Sectorization

The co-channel interference in a cellular system may be decreased by replacing omni-directional antennas with directional antennas, each radiating within a specified sector. Sectorization usually increases users' SINR or equivalently increases the system capacity, at the expense of increased numbers of antennas and decrease in trunking efficiency. The sectorizing antenna radiation pattern adopted in this paper is formulated as follows:

⁵ The cross-correlation terms can typically be discarded due to their insignificance (attenuated by a factor of spreading gain).

$$G_s(\theta) = \begin{cases} 1 - \frac{(1-b)}{(\pi/S)^2} \theta^2 & |\theta| \leq \sqrt{\frac{1-a}{1-b}} \frac{\pi}{S}, \\ a & \text{elsewhere} \end{cases} \quad (27)$$

where $G_s(\theta)$ is the gain of the antenna in a direction at angle θ relative to the maximal gain direction, a denotes the front-to-back ratio, b denotes the attenuation at sector crossover, and S is the number of sectors per cell. The antenna gain patterns for three and six sectors are given in Fig. 2 with $10 \log a = -15$ dB and $10 \log b = -3$ dB.

In our study, all techniques are employed in three-sector cells except the transmit diversity scheme, which is also studied in the six-sector cell case.

C. Beamforming Techniques

Before we discuss the various beamforming options, let us first assume generally a set of unit-norm transmit weighting vectors $\{\mathbf{w}_j\}_{j=1}^K$ are adopted for the K users' signals at the base station. On denoting $\mathbf{C}_j^i = [\mathbf{c}_j^{i1}, \dots, \mathbf{c}_j^{iL}]$, $\mathbf{h}_i = [\alpha_{i1}, \dots, \alpha_{iL}]^T$, and $\mathbf{l}_j^i = \mathbf{C}_j^i \mathbf{h}_i$, a standard space-time RAKE receiver of user i applied on (3) yields

$$z_i = (\mathbf{l}_i^i)^H \mathbf{r}_i = \sqrt{P_i} b_i \mathbf{w}_i^H \sqrt{G_i} \left(\sum_l \sum_{l'} \alpha_{il}^* \alpha_{il} (\mathbf{c}_i^{il'})^H \mathbf{c}_i^{il} \mathbf{a}_{il} \right) + \sum_{k \neq i} \sqrt{P_k} b_k \mathbf{w}_k^H \sqrt{G_i} \left(\sum_l \sum_{l'} \alpha_{il}^* \alpha_{il} (\mathbf{c}_i^{il'})^H \mathbf{c}_k^{il} \mathbf{a}_{il} \right) + \sum_{l=1}^L \alpha_{il}^* (\mathbf{c}_i^{il})^H \mathbf{n}_i. \quad (28)$$

With the assumption of

$$\langle \mathbf{c}_{k1}^{i,l1}, \mathbf{c}_{k2}^{i,l2} \rangle = \begin{cases} 1 & l1 = l2, k1 = k2 \\ 0 & l1 = l2, k1 \neq k2, \\ \beta & l1 \neq l2 \end{cases} \quad (29)$$

where β is a random variable defined in (20), and denoting

$$\mathbf{R}_i = G_i \sum_l \sum_{l'} |\alpha_{il}|^2 |\alpha_{il'}|^2 \mathbf{a}_{il} \mathbf{a}_{il'}^H \quad (30)$$

and

$$\mathbf{Q}_i = \frac{1}{N} G_i \sum_l \sum_{l' \neq l} |\alpha_{il}|^2 |\alpha_{il'}|^2 \mathbf{a}_{il} \mathbf{a}_{il'}^H, \quad (31)$$

the instantaneous SINR for user i is given by

$$\text{SINR}_i = \frac{P_i \mathbf{w}_i^H \left(\mathbf{R}_i + \mathbf{Q}_i + \frac{1}{N} G_i \sum_l \sum_{l' \neq l} |\alpha_{il}|^2 |\alpha_{il'}|^2 \mathbf{a}_{il} \mathbf{a}_{il'}^H \right) \mathbf{w}_i}{\sum_{k \neq i} P_k \mathbf{w}_k^H \mathbf{Q}_i \mathbf{w}_k + \sigma_i^2 \sum_l |\alpha_{il}|^2} \approx \frac{P_i \mathbf{w}_i^H \mathbf{R}_i \mathbf{w}_i}{\sum_{k \neq i} P_k \mathbf{w}_k^H \mathbf{Q}_i \mathbf{w}_k + \sigma_i^2 \sum_l |\alpha_{il}|^2}. \quad (32)$$

The power control formula (10) is exemplified here with

$$\mathbf{D} = \text{diag}(\gamma_1, \dots, \gamma_K), \quad (33)$$

$$F_{ij} = \begin{cases} 0 & i = j \\ \mathbf{w}_j^H \mathbf{Q}_i \mathbf{w}_j / \mathbf{w}_i^H \mathbf{R}_i \mathbf{w}_i & i \neq j \end{cases}, \quad (34)$$

and

$$u_i = \frac{\gamma_i \sigma_i^2 \sum_{l=1}^L |\alpha_{il}|^2}{\mathbf{w}_i^H \mathbf{R}_i \mathbf{w}_i}. \quad (35)$$

Since the downlink fading coefficients are not known at the base station, the approximation of Section II.B is adopted as follows:

$$\bar{\mathbf{R}}_i = G_i \sum_l \sum_{l'} E\{|\alpha_{il}|^2 |\alpha_{il'}|^2\} \mathbf{a}_{il} \mathbf{a}_{il'}^H, \quad (36)$$

and

$$\bar{\mathbf{Q}}_i = \frac{1}{N} G_i \sum_l \sum_{l' \neq l} E\{|\alpha_{il}|^2 |\alpha_{il'}|^2\} \mathbf{a}_{il} \mathbf{a}_{il'}^H, \quad (37)$$

where the expectation of the small-scale fading coefficients is estimated via time average from uplink data, and the downlink steering vectors are calculated through the estimated DOD, via DOA estimation from uplink data. Based on these matrices, various beamforming schemes are illustrated below. Equations (32) - (35) can be adjusted accordingly.

1) Beam Steering

This is a simple beamforming technique where the transmit antenna array forms a beam in the direction of line-of-sight of the desired user. It corresponds to the following antenna weights:

$$\mathbf{w}_i = \frac{\mathbf{a}^D(\theta_{i,los})}{\|\mathbf{a}^D(\theta_{i,los})\|}, \quad (38)$$

where $\theta_{i,los}$ denotes the azimuth angle of the line-of-sight of the i th user with the transmit antenna array.

2) Maximum SNR

This scheme maximizes the SNR at the i th user. According to (32), it is equivalent to

$$\arg \max_{\mathbf{w}_i} \mathbf{w}_i^H \bar{\mathbf{R}}_i \mathbf{w}_i. \quad (39)$$

It is well known that the solution to (39) is given by the principal eigenvector of the matrix $\bar{\mathbf{R}}_i$.

3) Maximum SIR/SINR

The maximum SIR scheme transmits as much energy as possible to the desired user while minimizing its interference to other users. Compared with its counterpart on uplink processing, there are two differences for the max SIR scheme: 1) the interference term is what this signal contributes to the other users, not that seen at the desired mobile; 2) the power levels of transmitted signals are not available at this stage (it is decided at the power control stage), so we cannot conduct maximum SINR as uplink processing. The maximum SIR scheme is formulated as

$$\arg \max_{\mathbf{w}_i} \frac{\mathbf{w}_i^H \bar{\mathbf{R}}_i \mathbf{w}_i}{\mathbf{w}_i^H \bar{\mathbf{T}}_i \mathbf{w}_i} \quad \text{with} \quad \bar{\mathbf{T}}_i = \sum_{k \neq i} \bar{\mathbf{Q}}_k. \quad (40)$$

Such \mathbf{w}_i is given by the generalized principal eigenvector of $[\bar{\mathbf{R}}_i, \bar{\mathbf{T}}_i]$. Compared to Max SNR, this criterion may lead to inadequate power being transmitted to the desired user, or equivalently, may lead to increased transmitted power that results in a type-II outage. Intuitively, there is no benefit in putting too much emphasis on interference minimization at the cost of reduced energy to the desired user, since the noise term cannot be eliminated.

In the packet-switched system, our goal is to maximize the network throughputs with the maximum transmit power, so the power allocation is known in advance. In this case, Max SINR can be exploited as follows:

$$\arg \max_{\mathbf{w}_i} \frac{\mathbf{w}_i^H \bar{\mathbf{R}}_i \mathbf{w}_i}{\mathbf{w}_i^H \bar{\mathbf{T}}_i \mathbf{w}_i} \quad \text{with} \quad \bar{\mathbf{T}}_i = \sum_{k \neq i} \bar{\mathbf{Q}}_k + \frac{K \sigma^2}{P_i} \mathbf{I}, \quad (41)$$

which can be seen as a tradeoff between the Max SNR and Max SIR schemes.

D. Joint Power Control and Maximum SINR Beamforming

The beamforming approaches given in the last subsection are not the optimum downlink beamforming. While uplink beamforming is a decoupled problem (a chosen weight vector impacts only the desired receiver), in transmit beamforming each transmit weighting affects all the receivers. So downlink beamforming should be done jointly for all users.

The joint power control and beamforming problem was first considered and solved in part in [14], [15], where the uplink joint algorithm is proposed and proved to converge to the optimal solution, and a feasible solution is obtained for the downlink through virtual uplink construction. A complete solution to the joint optimal power control and downlink beamforming is given in [18] through normalization with the noise term (see (32)):

$$\tilde{\mathbf{R}}_i = \frac{\bar{\mathbf{R}}_i}{\sum_l |\alpha_{il}|^2 \sigma_i^2} \quad \text{and} \quad \tilde{\mathbf{Q}}_i = \frac{\bar{\mathbf{Q}}_i}{\sum_l |\alpha_{il}|^2 \sigma_i^2}. \quad (42)$$

The optimization problem is given by

$$\min_{\substack{\mathbf{w}_1, \dots, \mathbf{w}_K \\ P_1, \dots, P_K}} \sum_{i=1}^K P_i \quad \text{s.t.} \quad \text{SINR}_i \geq \gamma_i \quad \text{and} \quad \|\mathbf{w}_i\| = 1, \quad (43)$$

with the SINR formula given by

$$\frac{P_i \mathbf{w}_i^H \tilde{\mathbf{R}}_i \mathbf{w}_i}{\sum_{k \neq i} P_k \mathbf{w}_k^H \tilde{\mathbf{Q}}_i \mathbf{w}_k + 1}. \quad (44)$$

The idea is to construct a *virtual uplink problem* with SINR

$$\frac{(P_i)_U \mathbf{w}_i^H \tilde{\mathbf{R}}_i \mathbf{w}_i}{\sum_{k \neq i} (P_k)_U \mathbf{w}_i^H \tilde{\mathbf{Q}}_k \mathbf{w}_i + \|\mathbf{w}_i\|^2}. \quad (45)$$

The following iterations converge to the optimal beamforming vector and power allocation from any initial values for the virtual uplink problem. (The superscript n means the n th iteration.)

Beamforming: For $1 \leq i \leq K$,

$$\mathbf{w}_i^n = \arg \max_{\mathbf{w}_i} \frac{\mathbf{w}_i^H \tilde{\mathbf{R}}_i \mathbf{w}_i}{\mathbf{w}_i^H \tilde{\mathbf{T}}_i^n \mathbf{w}_i}, \quad (46)$$

where

$$\tilde{\mathbf{T}}_i^n = \sum_{k \neq i} (\mathbf{p}_U^n)_k \tilde{\mathbf{Q}}_k + \mathbf{I}, \quad (47)$$

with $\mathbf{p}_U^n = [(P_1)_U^n, \dots, (P_K)_U^n]^T$ collecting the power at the n th iteration. This is the decentralized Max SINR scheme whose solution is the principal generalized eigenvector of $[\tilde{\mathbf{R}}_i, \tilde{\mathbf{T}}_i^n]$;

Power control:

$$\mathbf{p}_U^{n+1} = \tilde{\mathbf{D}}^n \tilde{\mathbf{F}}_U^n \mathbf{p}_U^n + \tilde{\mathbf{u}}_U^n, \quad (48)$$

where we define

$$\tilde{\mathbf{D}}^n = \text{diag} \left(\gamma_1 / (\mathbf{w}_1^n)^H \tilde{\mathbf{R}}_1 \mathbf{w}_1^n, \dots, \gamma_K / (\mathbf{w}_K^n)^H \tilde{\mathbf{R}}_K \mathbf{w}_K^n \right) \quad (49)$$

$$(\tilde{\mathbf{F}}_U^n)_{ij} = \begin{cases} 0 & i = j \\ (\mathbf{w}_i^n)^H \tilde{\mathbf{Q}}_j \mathbf{w}_i^n & i \neq j \end{cases} \quad (50)$$

and

$$(\tilde{\mathbf{u}}_U^n)_i = \frac{\gamma_i \|\mathbf{w}_i^n\|^2}{(\mathbf{w}_i^n)^H \tilde{\mathbf{R}}_i \mathbf{w}_i^n} = (\tilde{\mathbf{D}}^n \mathbf{1}_w^n)_i, \quad (51)$$

where

$$\mathbf{1}_w^n = [\|\mathbf{w}_1^n\|^2, \dots, \|\mathbf{w}_K^n\|^2]^T = \mathbf{1}. \quad (52)$$

This is the decentralized power control solution (see (11)) when the beamforming vector is fixed.

When the above algorithm converges, the optimal virtual uplink power vector is given by

$$\mathbf{p}_U = (\mathbf{I} - \tilde{\mathbf{D}}\tilde{\mathbf{F}}_U)^{-1}\tilde{\mathbf{u}}_U, \quad (53)$$

where $\tilde{\mathbf{D}}$, $\tilde{\mathbf{F}}_U$ and $\tilde{\mathbf{u}}_U$ are converged values of (49), (50) and (51), respectively.

In line with (50) and (51), we define

$$(\tilde{\mathbf{F}}^n)_{ij} = \begin{cases} 0 & i = j \\ (\mathbf{w}_j^n)^H \tilde{\mathbf{Q}}_i \mathbf{w}_j^n & i \neq j \end{cases} \quad (\text{i.e., } \tilde{\mathbf{F}}^n = (\tilde{\mathbf{F}}_U^n)^T) \quad (54)$$

and

$$(\tilde{\mathbf{u}}^n)_i = \frac{\gamma_i}{(\mathbf{w}_i^n)^H \tilde{\mathbf{R}}_i \mathbf{w}_i^n} = \tilde{\mathbf{D}}^n \mathbf{1} = (\tilde{\mathbf{u}}_U^n)_i. \quad (55)$$

Then we claim that the optimum downlink power vector is given by

$$\mathbf{p} = (\mathbf{I} - \tilde{\mathbf{D}}\tilde{\mathbf{F}})^{-1}\tilde{\mathbf{u}}, \quad (56)$$

where $\tilde{\mathbf{D}}$, $\tilde{\mathbf{F}}$ and $\tilde{\mathbf{u}}$ are converged values of (49), (54) and (55), respectively. This is because

$$\mathbf{1}^T \mathbf{p} = \mathbf{1}^T (\mathbf{I} - \tilde{\mathbf{D}}\tilde{\mathbf{F}})^{-1} \tilde{\mathbf{D}} \mathbf{1} = \mathbf{1}^T \tilde{\mathbf{D}} (\mathbf{I} - \tilde{\mathbf{D}}(\tilde{\mathbf{F}}_U)^T)^{-1} \mathbf{1} = (\mathbf{p}_U)^T \mathbf{1}, \quad (57)$$

so the optimality of \mathbf{p} is guaranteed by the optimality of the virtual uplink solution.

V. Numerical Results

In this section we examine the performance of the various downlink transmission techniques discussed above through computer simulation. For circuit-switched systems, power control is carried out and we evaluate and compare the supportable user capacity with certain SINR requirement under some outage limit. For the packet-switched system, we allow each base station to transmit at the maximum power and equally divide the power among the active users. We examine the cumulative distribution function of the SINR seen by a typical mobile user for performance comparison since the SINR is directly related to the achievable rate of the user. We also examine the effect of the optimal power assignment scheme of (9).

In our setting, the maximum transmitted power to background noise ratio (out-of-cell interference not included) is set to be 30 dB. The link SINR threshold is 5 dB for circuit-switched systems. The path loss parameter $\eta = 4$, and the standard deviation of the lognormal shadowing is 8 dB. The small-scale fading

coefficients are generated through the typical urban (TUx) model used in W-CDMA 3G studies [3]. The users are distributed uniformly within the sector of interest, with the antenna gain pattern given in Fig. 2. We assume that for each user there are three multipaths, the angles of which are Gaussian distributed around the direction of line-of-sight, with standard deviation of 10 degrees. The CDMA spreading gain is $N = 64$ for circuit-switched systems and $N = 8$ for packet-switched systems. The number of antennas M in our study is 2, 4, or 8 per sector. We assume each cell has three 120-degree sectors unless otherwise noted. When studying the transmit diversity scheme in the six-sector case, the number of users and antennas per sector is reduced to one half of those in the three-sector scenario.

A. Circuit-Switched System

Figures 3 to 5 present the performance of the six transmission techniques combined with power control for CDMA downlink circuit-switched systems, namely, transmit diversity, transmit diversity with sectorization, Max SNR beamforming, Max SIR beamforming, beam steering, and joint power control and (Max SINR) beamforming, in the form of supportable user capacity per sector⁶ with certain outage. We assume no feedback from the mobile. For the sake of comparison, the number of users that can be supported in one cell⁷ with 5% outage is given in Table 1, where the results of Max SNR beamforming and joint power control and beamforming with ideal feedback are also included. From these data, several conclusions can be made for CDMA downlink circuit-switched systems.

- We note that Max SNR beamforming approaches the optimal performance (that of joint power control and Max SINR beamforming) in the outage range of interest, while having much lower complexity, with or without instant downlink channel state information.
- For Max SNR beamforming, the gap between that with no feedback and that with feedback increases as the number of antennas increases, but for small numbers of antennas ($M = 2, 4$), the loss due to approximation of channel parameters is insignificant. This means that for small

⁶ per two sectors for transmit diversity with sectorization

⁷ three times the number in Figs. 3-5

numbers of antennas, Max SNR beamforming is the best choice even without feedback information.

- Max SIR has totally unacceptable performance and thus is omitted in Table 1. As we said before, putting too much emphasis on minimizing the interference to other users will hurt the desired energy; so more power has to be assigned to achieve the SINR threshold, resulting in type-II outage. Another problem with Max SIR is due to the insufficient degrees of freedom the antenna array can offer compared to the number of users for circuit-switched systems.
- Beam steering has good performance only when the number of antenna elements is small ($M = 2$); the gap between beam steering and Max SNR beamforming enlarges as M increases.
- For transmit diversity, sectorization significantly improves the performance (6 to 30 more users as M goes from 2 to 8 at 5% outage); but the Max SNR beamforming technique still outperforms the six-sector transmit diversity scheme (6 to 12 more users as M goes from 2 to 8 at 5% outage).

Figures 6 to 10 show the performance of the four transmission techniques as the number of antennas per sector varies from 2, 4 to 8 for circuit-switched systems. Max SIR beamforming is not of interest due to its unacceptable performance. The performance of joint power control and beamforming is similar to that of Max SNR and is omitted here. From these figures, the following conclusions can be drawn.

- For transmit diversity, the gain from exploiting more antennas *diminishes* as the number of antennas increases.
- For Max SNR beamforming the gain through exploiting more antenna elements *is restricted* due to imperfect channel knowledge. On the other hand, if we assume ideal feedback, the gain through exploiting more antenna elements *increases* with the number of antennas.
- For beam steering we observe an interesting phenomenon: the performance improves from $M = 2$ to $M = 4$, but deteriorates as M further increases. One possible explanation is that the beam steering scheme forms a beam toward the physical position of the mobile. Due to the angle spread model we use, it actually points in the wrong direction. As more antennas are used, more precise

calibration of the line-of-sight actually means greater angle estimation errors. This effect will counteract the benefit of antenna gains with more antennas.

B. Packet-Switched System

As a counterpart to the circuit-switched case, Figs. 11 to 13 present the performance of the six transmission techniques for packet-switched systems. We perform equal power assignment unless otherwise noted. The optimal power allocation combined with Max SNR serves as a performance baseline. In contrast with circuit-switched systems, we can implement the maximum SINR scheme here as we have knowledge of the power allocation. For the sake of comparison, the median (50% CDF) and peak (90% CDF) SINR values seen by a typical user are given in Table 2 and Table 3, respectively. Note that for the $M = 8$ and $K = 4$ case, the simultaneously transmitted users are doubled. One should consider this when translating SINR to achievable rates and network throughput. “(f)” in the tables designates results with feedback channel parameter information. From these data, several conclusions can be drawn for CDMA downlink packet-switched systems.

- Optimal power allocation has no benefit in packet-switched systems. We see from Figs. 11 to 13 that, the Max SNR with optimal power allocation, compared with Max SNR with equal power allocation, favors low-rate (low SINR) users but harms high-rate (high SINR) users. As we discussed in Section III, optimal power allocation is like a socialist scheme that seeks absolute fairness. It cannot achieve the highest throughput and, without being jointly considered with the link and network schedules, cannot guarantee fairness either. A similar phenomenon can be observed for the Max SINR scheme and is omitted here.
- Contrary to the circuit-switched case, Max SINR beamforming has the best performance in terms of peak rate; it is also good at median rate with small numbers of users, while comparable with others when there are more users.
- Max SNR beamforming is almost the best in terms of median rate; it is also good in terms of peak rate performance.

- Beam steering is almost as good as max SNR in terms of peak rate performance, while a little worse (1 dB) in terms of median rate performance.
- For transmit diversity, sectorization significantly improves the performance (4-7 dB).
- The Max SNR beamforming technique outperforms the six-sector transmit diversity scheme for $M = 8$ (1dB in median and 2-3 dB in peak); for $M = 4$, six-sector transmit diversity is better.

Figures 14 to 16 compare the performances of Maximum SINR beamforming with and without feedback. We find that feedback does not help much. Similar results hold for other beamforming techniques in packet-switched systems and are omitted here.

VI. Conclusions

In this paper, we have seen that traffic type impacts the algorithm choice in CDMA cellular downlink transmission with antenna arrays in multipath fading channels. For circuit-switched downlink CDMA systems, the Max SNR beamforming scheme is the best choice (accommodating 12 to 42 more users than transmit diversity). For packet-switched systems, Max SINR Beamforming has the best performance in terms of peak rate (10-14 dB more than transmit diversity); Max SNR beamforming is almost the best in terms of median rate (3-4 dB more than transmit diversity), but beam steering and transmit diversity with sectorization are also good choices. Optimum power control/allocation schemes have been shown to be either too complex or infeasible in practice. In circuit-switched systems, the gap between the performance with no feedback channel information and that with feedback increases as the number of antennas increases, but for small numbers of antennas, the loss due to approximation of channel parameters is insignificant. On the other hand, feedback channel information does not help much for beamforming techniques in packet-switched systems. We also see that sectorization greatly improves the system performance, both for the circuit-switched and for the packet-switched systems.

The following issues deserve further study in this context. In this paper, we have assumed the perfect knowledge of the DOD when calculating the downlink spatial covariance matrix. The issue of parameter estimation errors in covariance matrix calculation is of interest. Other interesting topics include joint

consideration of link and network schedules with transmission techniques in packet-switched systems, and array-processing techniques to combat the large-scale fading exploiting widely separated antennas (macrodiversity).

Acknowledgement: The authors would like to thank Drs. Dmitry Chizhik, Constantinos Papadias, Jerry Foschini, Mike Gans, Howard Huang, Jack Salz, Reinaldo Valenzuela and all other members of the Wireless Communications Research Department of Bell Labs, Lucent Technologies, for helpful discussions. Part of this work was done while Huaiyu Dai was a summer intern there.

Bibliography

- [1] T. Aste et al., "Downlink beamforming avoiding DOA estimation for cellular mobile communications," *Proc. 1998 IEEE Int. Conf. Acoust. Speech, Sig. Process.*, pp. 3313-3316, Seattle, Washington, May 1998.
- [2] G. J. Foschini, "A simplified distributed autonomous power control algorithm and its convergence," *IEEE Trans. Veh. Technol.*, vol. 42, no. 4, pp. 641-646, Nov. 1993.
- [3] V. K. Garg, *IS-95 CDMA and cdma2000*, Upper Saddle River, NJ: Prentice Hall PTR, 2000.
- [4] R. Gejji, "Forward-link-power control in CDMA cellular systems," *IEEE Trans. Veh. Technol.*, vol. 41, no. 4, pp. 532-536, Nov. 1992.
- [5] G. H. Golub and C. F. Van Loan, *Matrix Computation*, The John Hopkins University Press, Baltimore, MD, 1996.
- [6] S. Hanly and D. Tse, "Power control and capacity of spread spectrum wireless networks," *Automatica* 35, pp. 1987-2012, 1999.
- [7] B. Hochwald, T. Marzetta and C. Papadias, "A transmitter diversity scheme for CDMA systems based on space-time spreading," *Bell Labs Technical Memorandum*, May 1999.
- [8] B. Hochwald and T. Marzetta, "Adapting a downlink array from uplink measurements," *Bell Labs Technical Memorandum*, Feb. 1999.
- [9] H. Huang, "Increasing IS-95 downlink capacity with transmit and receive diversity," *Bell Labs Technical Memorandum*, Nov. 1997.
- [10] H. Minc, *Nonnegative Matrices*, New York: Wiley, 1988.
- [11] J. Paulraj and C. B. Papadias, "Space-time processing for wireless communications," *IEEE Signal Processing Mag.*, pp. 49-82, Nov. 1997.
- [12] G. Raleigh et al., "A blind adaptive transmit antenna algorithm for wireless communications," *Proc. 1995 IEEE International Conf. on Communications*, pp. 1494-1499, Seattle, WA, June 1995.
- [13] T. S. Rappaport, *Wireless Communications: Principles and Practice*, Second Edition, Upper Saddle River, NJ: Prentice Hall PTR, 2002.
- [14] F. Rashid-Farrokhi et al., "Joint optimal power control and beamforming in wireless networks using antenna arrays," *IEEE Trans. Commun.*, Vol. 46, no. 10, pp. 1313-1324, Oct. 1998.
- [15] F. Rashid-Farrokhi et al., "Transmit beamforming and power control for cellular wireless systems," *IEEE Select. Areas Commun.*, vol. 16, no. 8, pp. 1437-1449, Oct. 1998.
- [16] B. D. Van Veen and K. M. Buckley, "Beamforming: a versatile approach to spatial filtering," *IEEE ASSP Mag.*, vol. 5, pp. 4-24, Apr. 1988.
- [17] S. Verdú, *Multiuser Detection*, Cambridge, UK: Cambridge University Press, 1998.
- [18] E. Visotsky and U. Madhow, "Optimal Beamforming Using Transmit Antenna Arrays," *Proc. 1999 Spring IEEE Vehicular Technology Conf.*, pp. 851-856, Houston, TX, May 1999.
- [19] S. Wang and I. Wang, "Effects of soft handoff, frequency reuse and non-ideal sectorization on CDMA system capacity," *Proc. 1993 Spring IEEE Vehicular Technology Conf.*, pp. 850-854, Secaucus, NJ, May 1993.

- [20] X. Wang and H. V. Poor, "Space-time multiuser detection in multipath CDMA channels," *IEEE Trans. Signal Processing*, vol. 47, no. 9, pp. 2356-2374, Sept. 1999.
- [21] J. H. Winters, J. Salz and R. D. Gitlin, "The impact of antenna diversity on the capacity of wireless communication systems," *IEEE Trans. Commun.*, Vol. 42, no. 2/3/4, pp. 1740-1750, Feb./Mar./Apr. 1994.
- [22] A. Wyner, "Shannon-theoretic approach to a Gaussian cellular multiple-access channel," *IEEE Trans. Inform. Theory*, vol. 40, no. 6, pp.1713-1727, Nov. 1994.
- [23] W. Yang and G. Xu, "Optimal Downlink Power Assignment for Smart Antenna Systems," *Proc. 1998 IEEE Int. Conf. Acoust. Speech, Sig. Process.*, pp. 3337-3340, Seattle, Washington, May 1998.

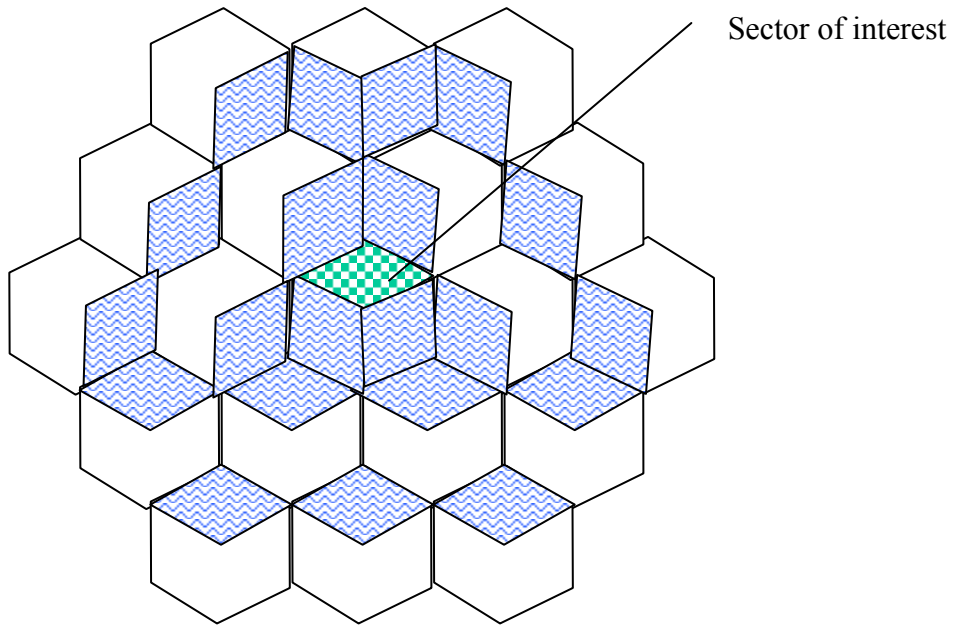


Fig. 1 Cellular simulation model

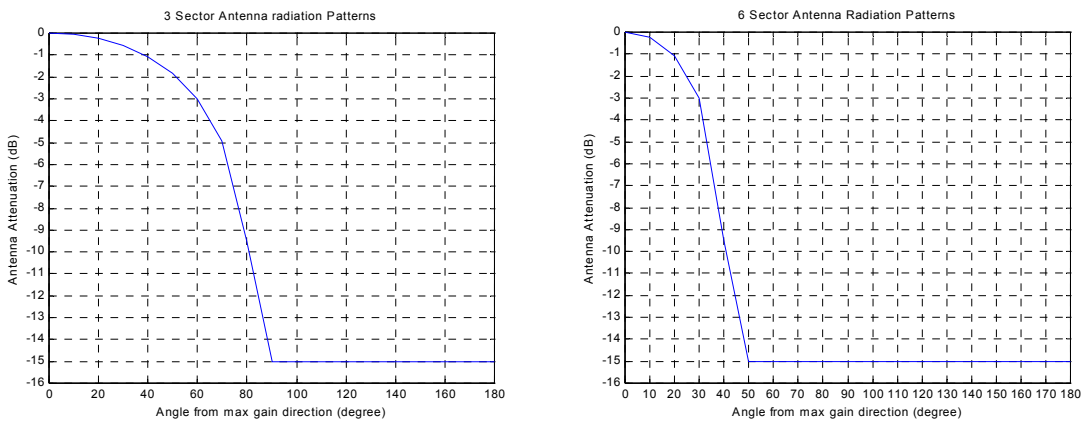


Fig. 2 Sector antenna radiation pattern

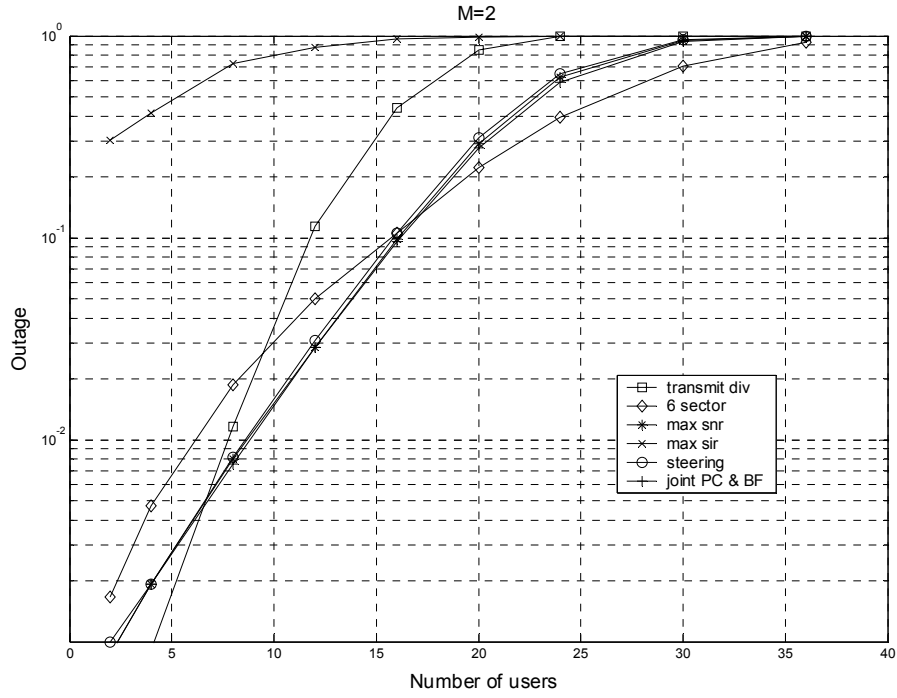


Fig. 3 Performance comparison of various transmission techniques with $M = 2$ antennas per sector (6 antennas per cell) — circuit-switched system

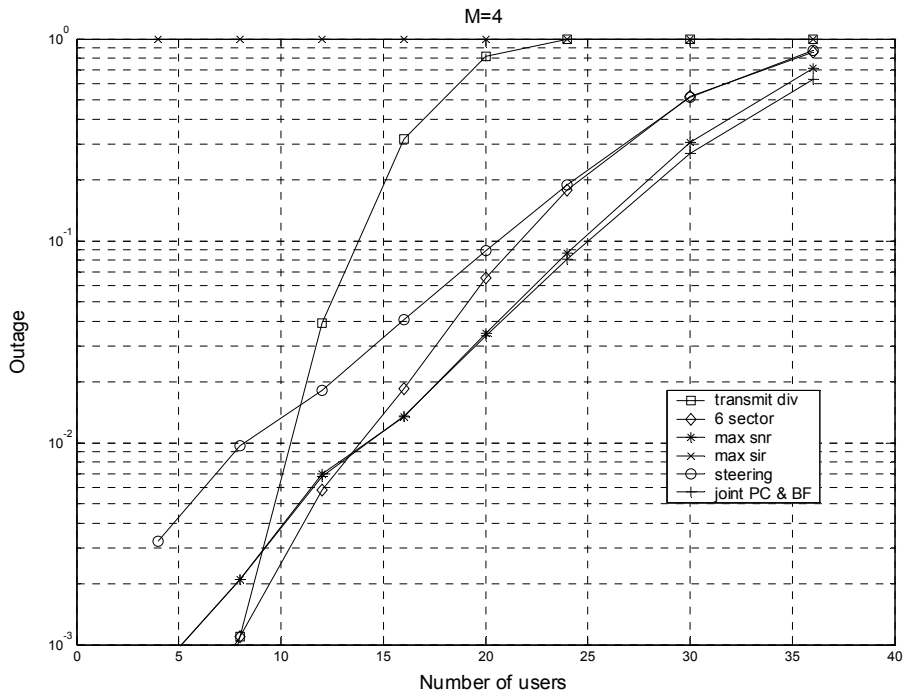


Fig. 4 Performance comparison of various transmission techniques with $M = 4$ antennas per sector (12 antennas per cell) — circuit-switched system

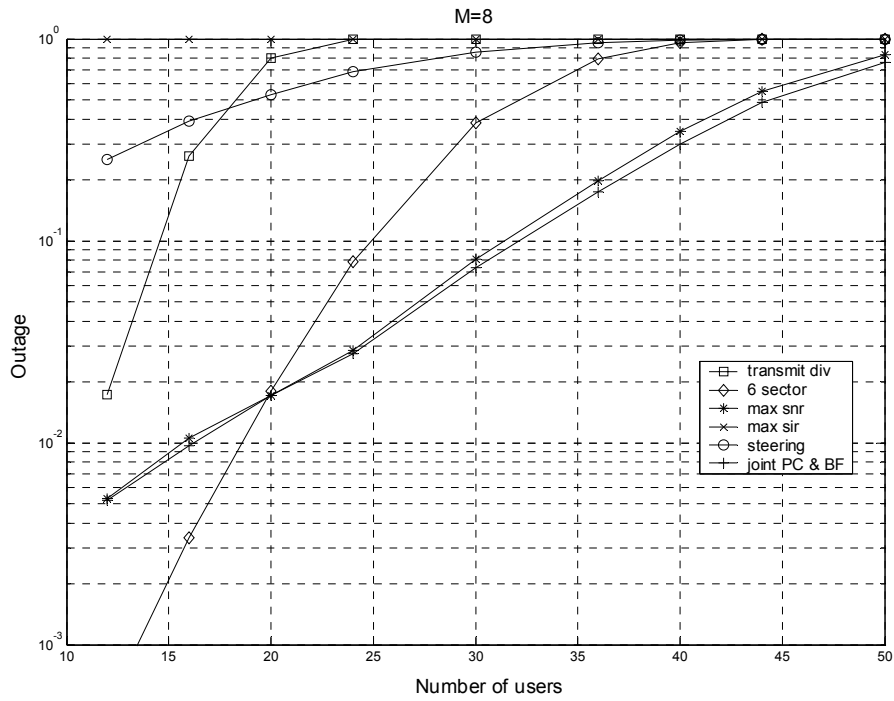


Fig. 5 Performance comparison of various transmission techniques with $M = 8$ antennas per sector (24 antennas per cell) — circuit-switched system

Table 1 Number of users supported in a cell with 5% outage

Transmit Diversity	Six Sector	Beam Steering	Max SNR	Max SNR with feedback	Joint	Joint with feedback	
30	36	39	42	42	42	42	→ 6 antennas per cell
36	57	51	66	72	66	72	→ 12 antennas per cell
39	69	12	81	117	84	117	→ 24 antennas per cell

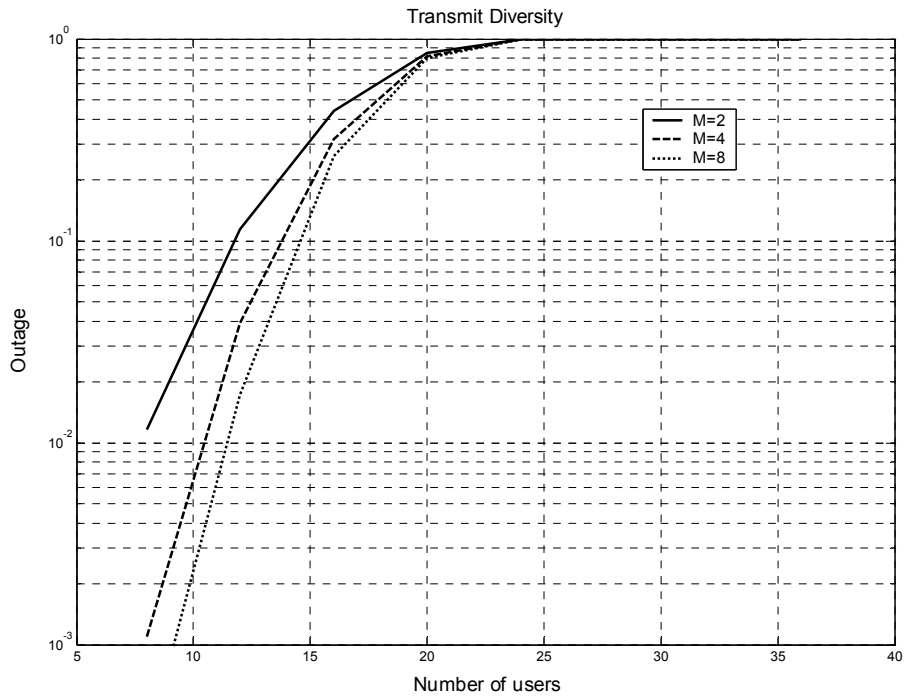


Fig. 6 Performance of transmit diversity with 2, 4 and 8 antennas per sector

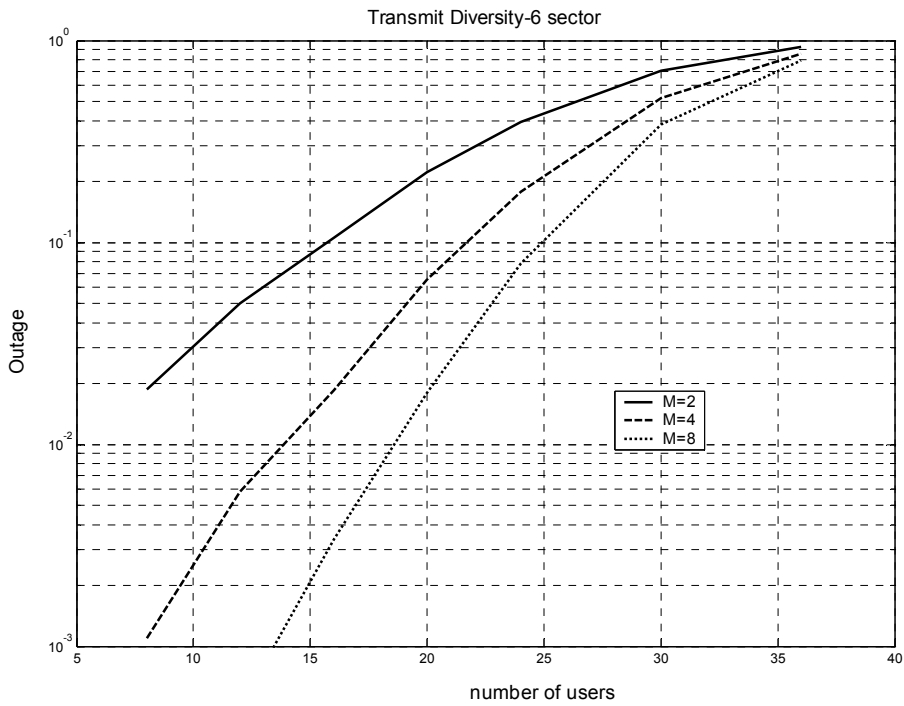


Fig. 7 Performance of transmit diversity with sectorization with 2, 4 and 8 antennas per sector

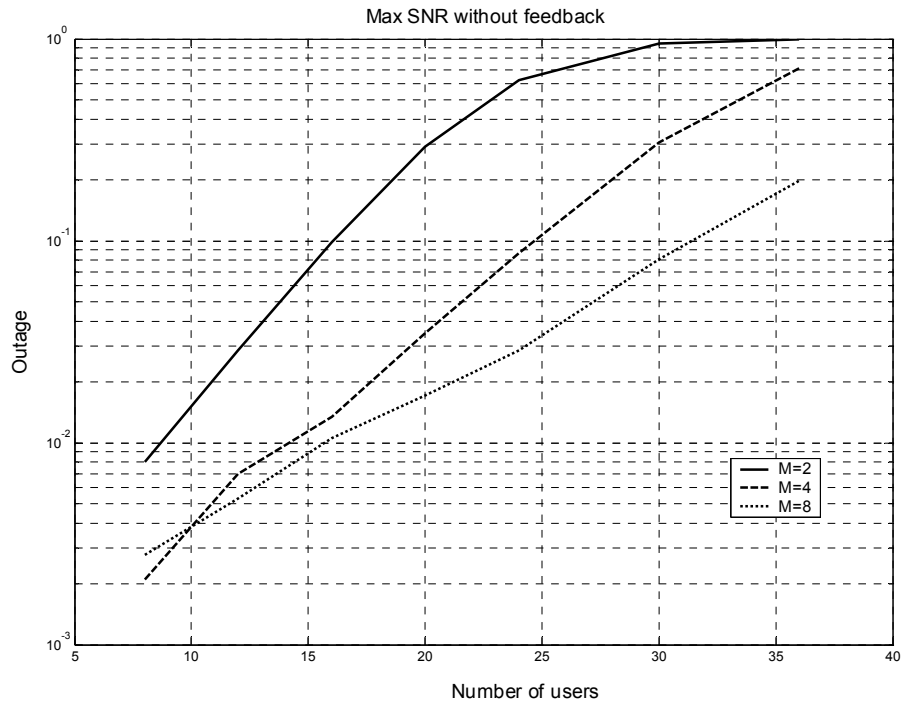


Fig. 8 Performance of max SNR beamforming without feedback with 2, 4 and 8 antennas per sector

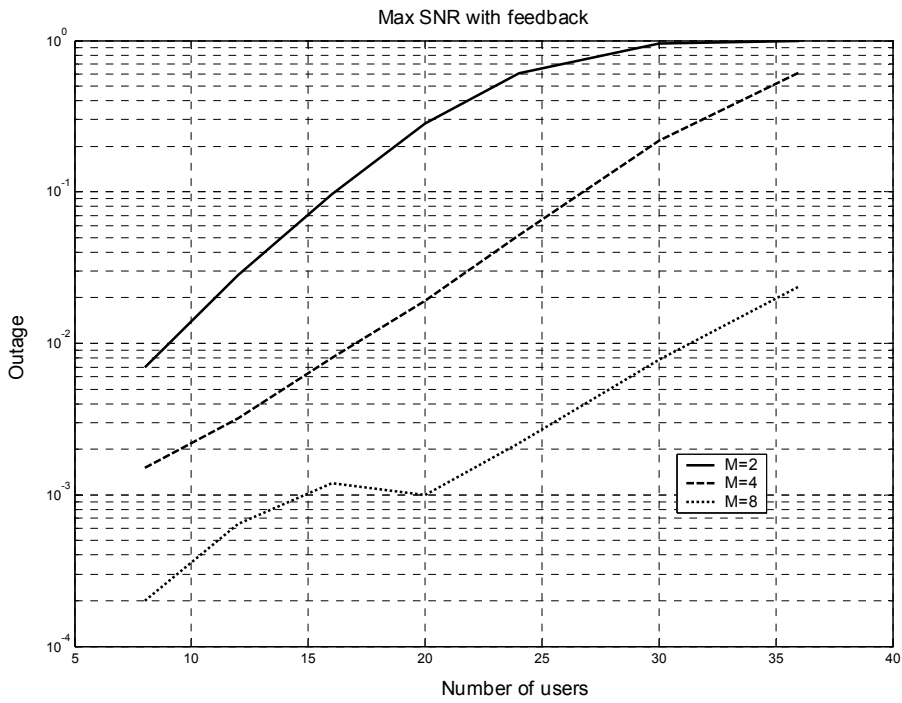


Fig. 9 Performance of max SNR beamforming with feedback with 2, 4 and 8 antennas per sector

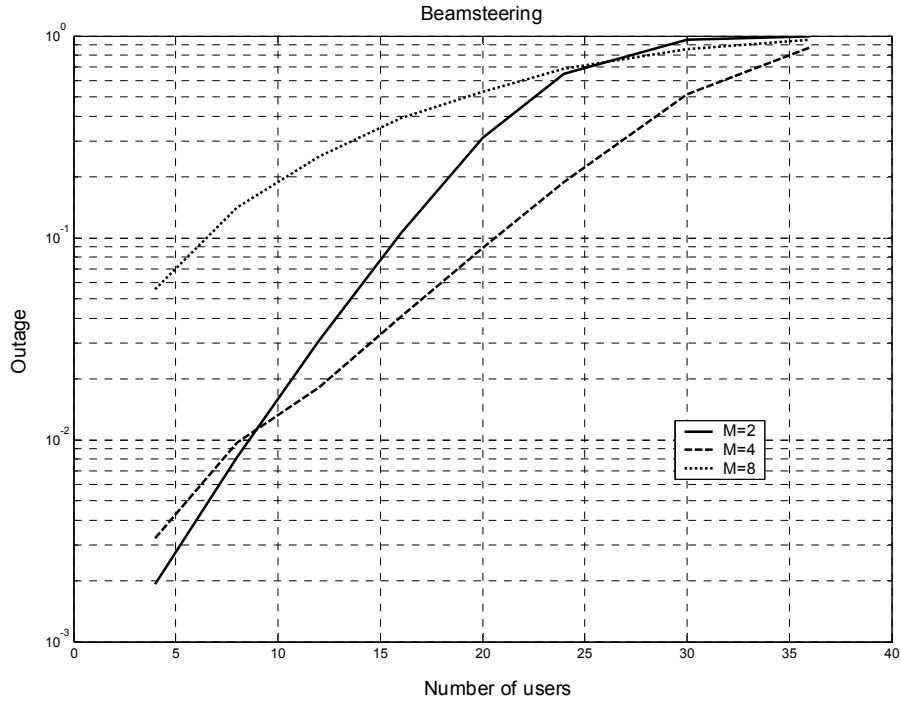


Fig. 10 Performance of beam steering with 2, 4 and 8 antennas per sector

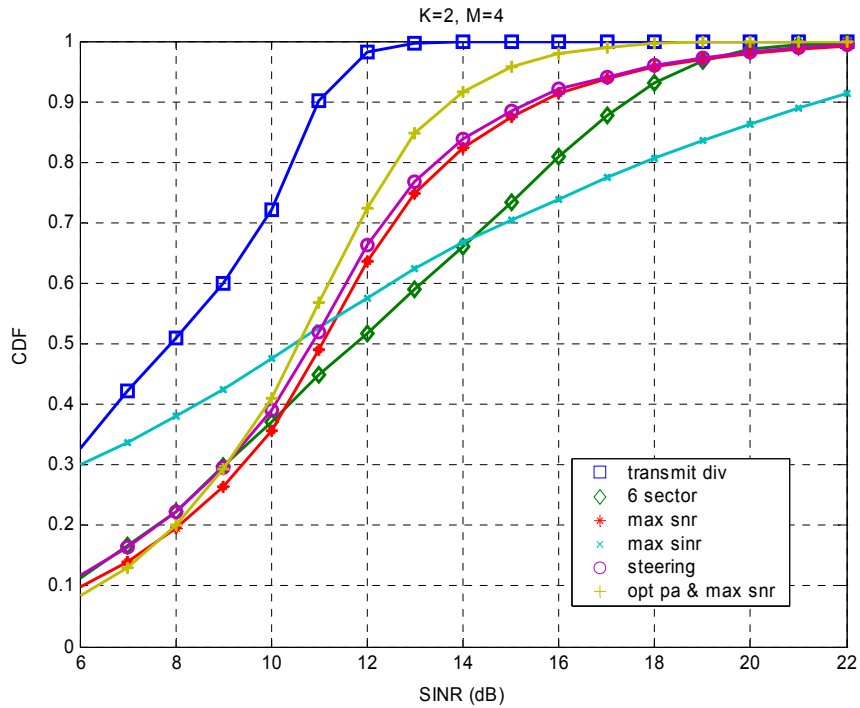


Fig. 11 Performance comparison of various transmission techniques with $M = 4$ antennas and 2 active users — packet-switched system

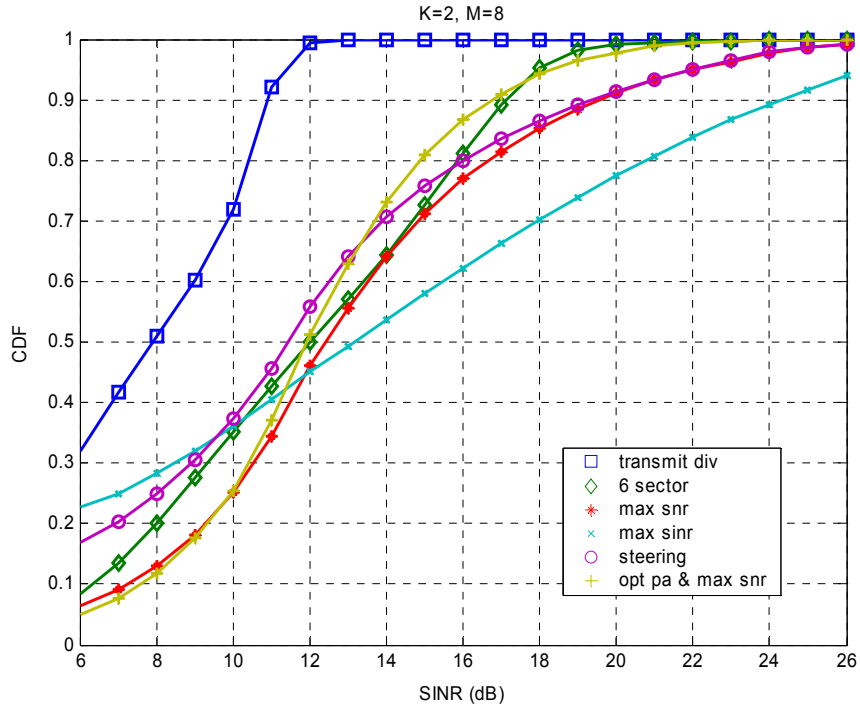


Fig. 12 Performance comparison of various transmission techniques with $M = 8$ antennas and 2 active users — packet-switched system

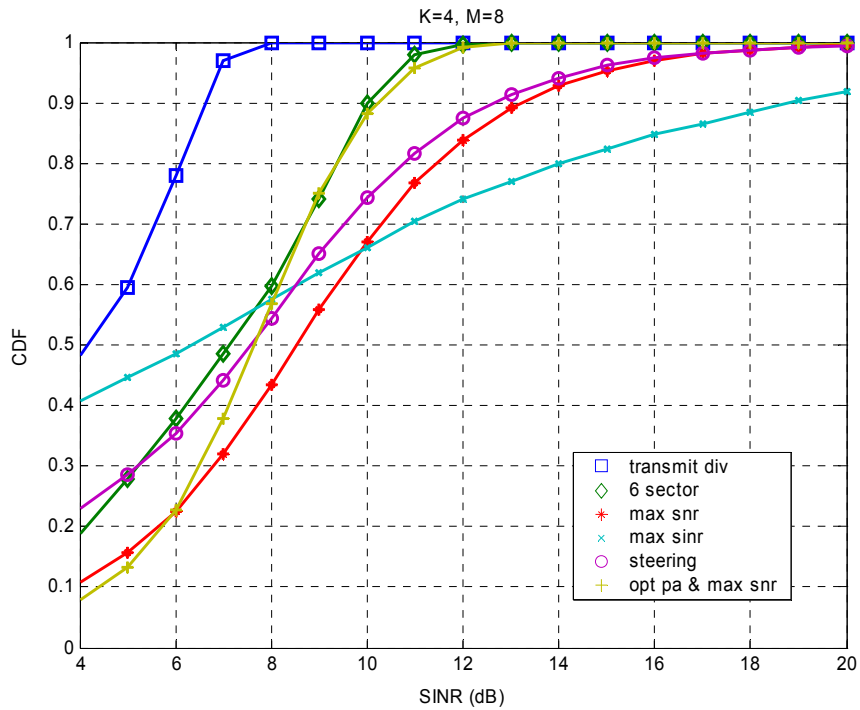


Fig. 13 Performance comparison of various transmission techniques with $M = 8$ antennas and 4 active users — packet-switched system

Table 2 Median SINR (50% CDF) of a typical mobile user (dB)

Transmit Diversity	Six Sector	Beam Steering	Max SNR	Max SNR(f)	Max SINR	Max SINR(f)	Opt PA & Max SNR	Opt PA & Max SINR(f)	
8	11.8	10.8	11	11.1	10.6	10.8	10.6	10.7	$M=4 \text{ \& } K=2$
8	12	11.4	12.4	12.7	13.2	13.7	11.9	12.3	$M=8 \text{ \& } K=2$
4.2	7.2	7.6	8.5	8.8	6.4	7.2	7.7	8.2	$M=8 \text{ \& } K=4$

Table 3 Peak SINR (90% CDF) of a typical mobile user (dB)

Transmit Diversity	Six Sector	Beam Steering	Max SNR	Max SNR(f)	Max SINR	Max SINR(f)	Opt PA & Max SNR	Opt PA & Max SINR(f)	
11	17.5	15.5	15.7	15.7	21.6	21.6	13.8	13.8	$M=4 \text{ \& } K=2$
10.8	17.2	19.3	19.5	19.5	24.3	24.6	16.8	17.1	$M=8 \text{ \& } K=2$
6.8	10	12.7	13.3	13.4	18.8	19.3	10.3	10.6	$M=8 \text{ \& } K=4$

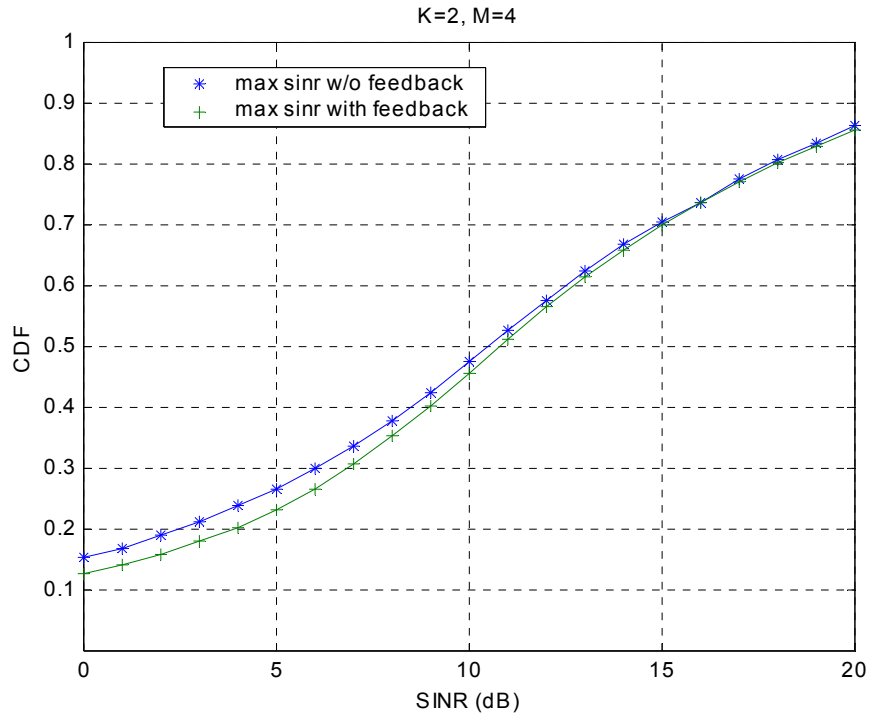


Fig. 14 Performance of max SINR beamforming with 4 antennas and 2 active users: with and without feedback channel information

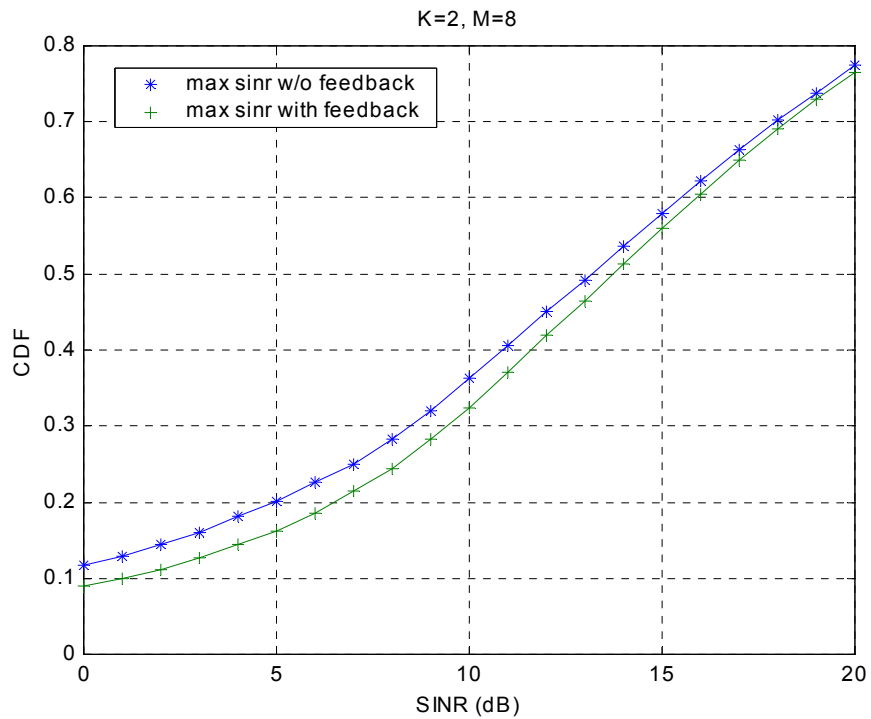


Fig. 15 Performance of max SINR beamforming with 8 antennas and 2 active users: with and without feedback channel information

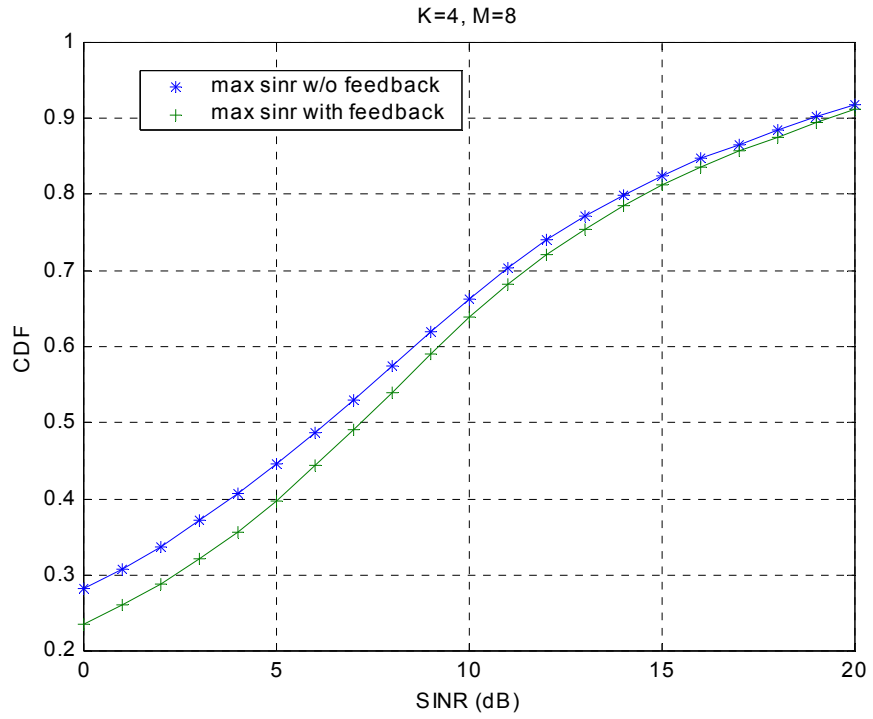


Fig. 16 Performance of max SINR beamforming with 8 antennas and 4 active users: with and without feedback channel information